JAM CM Journal of Applied Mathematics and Computational Mechanics 2023, 22(4), 18-29
www.amcm.pcz.pl p-ISSN 2299-9965
DOI: 10.17512/jamcm.2023.4.02 e-ISSN 2353-0588

CRITICAL LOADING OF PILLAR ARRAYS HAVING PREVIOUSLY ELIMINATED ELEMENTS

Tomasz Derda

Department of Mathematics, Czestochowa University of Technology
Czestochowa, Poland
tomasz.derda@pcz.pl

Received: 30 September 2023; Accepted: 6 December 2023

Abstract. The paper analyzes critical loads of pillar arrays with fraction of elements removed prior to actual critical loading. Two different methods of elimination are considered. In the first case, a fraction p of weakest pillars is physically removed from the array. The second method relies on conducting a subcritical preloading. When the sudden loading is applied to the system, the destruction follows in a cascade-like manner. Subsequent cascades take place due to the redistribution of load. We explore different types of load redistribution. It turns out that the type of load transfer as well as the distribution of pillar-strength-thresholds are of crucial importance regarding the strength enhancement of critically loaded pillar arrays.

MSC 2010: *82D30, 82D80, 65Z05*
Keywords: *fiber bundle model, load transfer, multicomponent system, strength enhancement*

1. Introduction

Arrays of pillars are examples of electro-mechanical multicomponent systems. Especially over the last years, arrays of micro/nanopillars have attracted increasing attention within research community [1]. Due to the small feature size and periodicity of the structure, micro/nanopillar arrays have unique properties allowing applications in nanotechnology. They are encountered, e.g., in sensors, optical devices or energy generation devices [2].

Multiple uniaxial tensile and compressive experiments prove that sub-micron-scale metallic pillars have enhanced strength compared to their bulk counterparts [3, 4]. However, micro- and nanomaterials usually display sample-to-sample fluctuations [5]. Therefore, a system of individual pillars gathered together into an array also exhibits sample-to-sample fluctuations when subjected to an external load. The load carrying capacity of such system is a random variable known only through its probability distribution.

In our study, a multicomponent system consists of a multitude of pillars. Although the pillars are functionally identical, they differ in their strength thresholds. To model

the loading process of the array, the Fibre Bundle Model approach is applied [6, 7]. When the array of vertically aligned pillars is axially loaded, pillars whose strength-thresholds are smaller than loads locally imposed on them fail. Then, the loads from the destroyed pillars are redistributed to the ones that remain intact. The ultimate strength of the system is dependent not only on the distribution of pillar-strength--thresholds [8, 9], but also on the type of load transfer [10, 11], loading conditions [12,13] and method of loading. Generally, the loading process can be divided into two methods: sudden loading and quasi-static loading. The other possibility is conducting a cyclic loading. It turns out that after carefully tuned low-amplitude cyclic loading, a single sub-micron pillar obtains a significantly higher strength [14, 15]. Numerical simulations show that application of optimally tailored cyclic preloading on pillar arrays induces noticeable strengthening of the system, even though some of the pillars may be destroyed during precompression [16]. Inspired by this, we are interested in the effect of elimination of some pillars from the system done prior to actual critical loading. However, we assume that pillar-strength-thresholds remain quenched during the whole process. The elimination of some fraction of pillars is accomplished by one of the two methods described in the next section.

In the following, in Section 2, we provide description of our model, including two ways of pre-elimination of the elements from the system. The results of numerical simulations are presented in Section 3. Finally, we briefly summarize our findings.

2. Arrays of pillars under critical sudden loading

Initially, the system is composed of $N = L \times L$ pillars located at nodes of a square substrate, where L is a linear system size. Strength-thresholds of pillars are independent and identically distributed random variables. Therefore, the load carrying capacity of the system is random as well. Each pillar is seen as a two-state component, either intact or crushed. The term 'intact' means that the pillar is fully functional. When the load applied locally on the pillar attains its strength-threshold, the pillar instantaneously and irreversibly collapses. The crushed/eliminated pillar carries no load.

As the pillar-strength-thresholds σ_{th} are random variables, we employ two probability distribution functions: uniform distribution on the interval $[0,1]$ and two--parameter Weibull distribution whose cumulative distribution function is as follows

$$P_{\rho,\lambda}(\sigma_{th}) = 1 - \exp\left[-(\sigma_{th}/\lambda)^{\rho}\right] \tag{1}$$

where ρ is a shape parameter and λ is a scale parameter. We assume that $\lambda = 1$. Shape parameter ρ characterizes the amount of threshold disorder.

In the sudden loading process, a total load F is suddenly applied on the entire system. Suppose that at the beginning of the loading process the number of intact pillars is equal to N_0 $(N_0 \leq N)$. The external loading is uniform, hence a load per pillar takes the value of $f_0 = F/N_0$. All the pillars whose $\sigma_{th} \leq f_0$ become crushed,

whereas the rest of the loaded pillars remain intact. The initial breaking is followed by redistribution schemes that lead the system either to a complete failure or to a stable state of partial destruction. Hence, the whole process runs in a self-sustained cascade--like manner triggered by initial breaking. The total external load is fixed during the process. Each cascade can be seen as a time step, then the total number of cascades corresponds to a relaxation time τ.

The loads released by the crushed pillars are redistributed to the intact components according to a given transfer rule. There are two extreme load transfer rules, namely global load sharing (GLS) and local load sharing (LLS). The GLS rule corresponds to a perfectly rigid substrate – the load from a destroyed pillar is transmitted equally to all intact elements in the system irrespective of their distance from the crushed one. This rule represents mean-field approximation. In the case of the GLS rule, the effective range of interaction is infinite – all the intact pillars receive the same load increment. This is in contrast to the LLS rule, where short interactions are observed – only the nearest intact neighbours of the crushed pillar suffer additional load. It is assumed here that pillars are placed on a non-rigid substrate that has a nonvanishing compliance.

The rule of load transfer that interpolates between above-mentioned extreme ones bases on a power-law redistribution [10, 11]. This rule is called a range variable (RV) load transfer rule. In this case, the load ΔQ_i carried by the crushed i-th pillar is transferred to all intact pillars in the system according to the formula

$$\frac{Z_i}{|r_j - r_i|^{\gamma}} \Delta Q_i \tag{2}$$

where γ is an adjustable parameter ($\gamma \geq 0$), $|r_j - r_i|$ is a distance between crushed i-th and intact j-th pillars, and Z_i is a normalization factor that provides conservation of load. The GLS rule is equivalent to the RV rule with $\gamma = 0$. By increasing the value of the parameter γ, we are reducing the effective range of interactions. Hence, when $\gamma \to \infty$, the RV rule operates like the pure LLS system. The characteristic feature of the RV scheme is that all the intact pillars are affected by the load coming from the crushed one, although not in the same proportion (excluding $\gamma = 0$). We also note that redistribution of load for $\gamma \gg 0$ (as well as for the LLS rule) leads to inhomogeneities in load carried by individual pillars.

In this work, we analyze the effect of the elimination of some fraction of pillars before the actual critical loading process. This elimination is realized by one of the two methods, namely:

- fraction p of weakest components is physically eliminated from the system,
- random fraction of the components is removed from the system by carrying out the subcritical preloading.

Under the first method, we assume that a fraction p of weakest pillars is removed from the system prior to critical loading. The nodes in which the removed components were placed remain empty during critical loading. The empty nodes are treated

as nodes of pillars crushed during the loading process i.e., they carry no load. By varying the fraction p from 0 to 0.8, we can pass from dense arrays to sparse arrays.

Applying the second method, we investigate how the strength of array is influenced by subcritical precompression. Each array is characterized by its own subcritical load, being a random variable. We are aware that both analyzed methods are theoretical, but they allow us to capture the qualitative effect of elimination of weak elements from the system.

3. Simulation results

Based on the model described in the previous section, we have built up Wolfram Mathematica codes to adequately simulate the loading processes. In order to obtain reliable results, we have carried out a substantial number of simulations. We went from $N = 40 \times 40$ to $N = 350 \times 350$ – such a range allows us to gain insight into possible size effects. We have exploited uniform distribution as well as Weibull distribution of pillar-strength-thresholds. For the latter, we have chosen $\rho = 2, 5, 8$ – these values ensure passing from high to low disorder of pillar-strength-thresholds.

For each configuration, at least $M = 5 \times 10^3$ sets of samples $\{\sigma_{th}\}^{(i)}$, $i \in \{1, \ldots, M\}$ are randomly created before the simulations of loading. Then, taking samples one by one, we have conducted loading experiments.

We define the ultimate strength of the system $F_{\max}$ as the maximum external load F sustained by the system, i.e. the system is in a stable state with only a fraction of destroyed elements. Our model is not time-dependent, hence we neglect that even a subcritical load can provoke failure of the entire system. To facilitate comparison of arrays of different sizes, the strength is scaled by a corresponding value of N: $f_{\max} = F_{\max}/N$.

Adding even a small amount of load (per pillar) δ to the subcritical load $f_{\max}$ results in a collapse of the system. Thus, $f_c = f_{\max} + \delta$ is a critical load of the system – minimum suddenly applied load under which the system is down. In our simulations, the condition $\delta \leq \min(0.0001, 1/N)$ is satisfied. It should be noted that the total critical load equals to $F_c = f_c N$.

3.1. The effect of removing fraction p of the weakest pillars

As it was previously mentioned, we tune the fraction p by varying it between $p = 0$ and $p = 0.8$ with a step of 0.02. Therefore, at the beginning of the critical loading process, the number of intact elements is equal to $N_p = (1 - p)N$. Thus, to induce catastrophic avalanche of self-sustained cascades of pillar crushes, the critical load $f_c N/N_p$ has to be uniformly applied on all intact components. It is noted that, assuming fixed f_c, the increasing of p causes the growing of initial load imposed locally on the intact pillars. However, such locally increased load is applied to the array that is devoid of weakest elements. The effect of a decreasing population of

weak components is especially interesting in the case of the LLS-like rule where catastrophic avalanche propagates in a form of clusters of crushed pillars initiated in weak regions. The probability of finding a weak region of intact elements is a decreasing function of p. However, from a certain value of p, the array becomes too sparse to indicate enhanced strength.

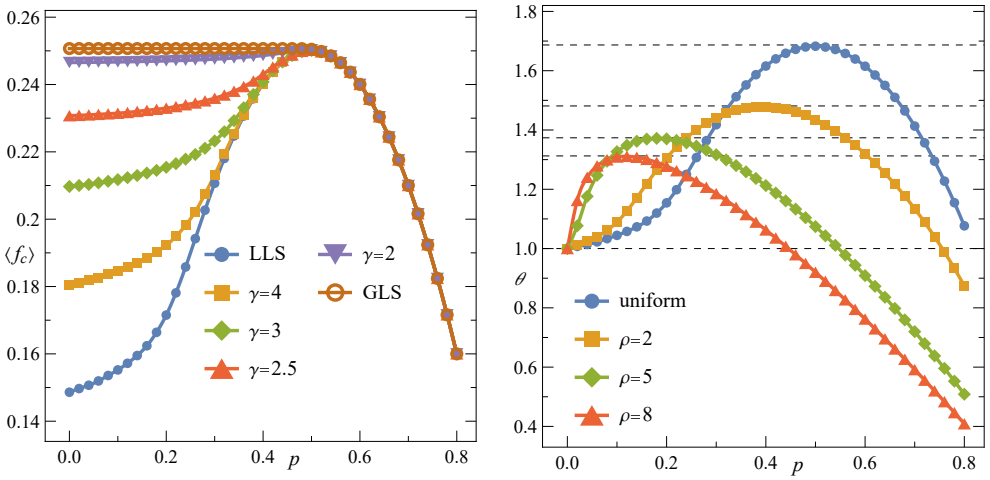

Fig. 1. (Left panel) Mean critical load $\langle f_c \rangle$ vs. fraction p. Systems with uniformly distributed pillar-strength-thresholds. (Right panel) Mean strengthening/weakening of the LLS systems for different types of distribution of pillar-strength-thresholds. Four upper dashed lines correspond to ratio $\langle f_c^{\mathrm{GLS}}(p=0)\rangle / \langle f_c^{\mathrm{LLS}}(p=0)\rangle$ for uniform distribution, $\rho = 2$, $\rho = 5$ and $\rho = 8$ (from up to down). Both panels concern results for systems of initial size $N = 100 \times 100$

The left panel of Figure 1 reports values of empirical mean critical loads $\langle f_c \rangle$ as a function of p for different types of load redistribution. It is seen, in the case of the GLS rule, that values of $\langle f_c \rangle$ remain almost constant up to $p_c \approx 0.5$, and then they start to decrease. Hence, in the mean-field-like approach with uniformly distributed strength-thresholds, removal of up to 50 percent of the weakest pillars does not affect the mean strength of the system. Similar behaviour is observed in the case of Weibull distribution, however the transition points are different: $p_c \approx 0.4$ for $\rho = 2$, $p_c \approx 0.18$ for $\rho = 5$ and $p_c \approx 0.12$ for $\rho = 8$. Therefore, in the GLS systems, the smaller the disorder is, the bigger the fraction of strongest pillars will need to be to support $f_{\max}(p) \approx f_{\max}(p=0)$.

Another observation coming from the analyzed data is as follows: mean critical loads for the other load transfer rules tend to the GLS one, as the fraction p increases (see left panel of Fig. 1). Especially, in the case of the LLS rule the mean critical load grows quite sharply to reach the value of its GLS counterpart at $p_c \approx 0.5$ (uniform distribution). When all the other systems converge to the GLS system at its transition point p_c, the values of $\langle f_c \rangle$ start to go down. From the transition point, the applied load transfer rule is irrelevant, as all the systems behave like the GLS one. By increasing the fraction p, the density of occupied nodes decreases, and thus the effective range of the short range interactions grow.

Table 1. Data corresponding to maximum strengthening for chosen examples

Initial system size N	Load transfer	Max ratio $\frac{\langle f_c(p)\rangle}{\langle f_c(p=0)\rangle}$	Fraction p
uniform			
100×100	$\gamma=2$	1.015	0.50
	$\gamma=2.5$	1.084	0.50
	$\gamma=3$	1.193	0.50
	$\gamma=4$	1.386	0.50
	$\gamma=10$	1.663	0.50
	LLS	1.683	0.50
$\rho=2$			
60×60	LLS	1.420	0.40
100×100	LLS	1.478	0.40
140×140	LLS	1.517	0.40
$\rho=5$			
100×100	LLS	1.371	0.18
$\rho=8$			
100×100	LLS	1.311	0.12

We define the ratio $\theta(p)=\langle f_c(p)\rangle/\langle f_c(p=0)\rangle$ as the mean strengthening ($\theta>1$) or weakening ($\theta<1$) of the system. The scale of strengthening/weakening for the LLS systems is visible in the right panel of Figure 1. Systems with uniformly distributed pillar-strength-thresholds are strengthened even in the case of sparse arrays ($p=0.8$). Taking into consideration Weibull distribution, we notice that the degree of strengthening is strongly dependent on the type of distribution of strength--thresholds: the maximum strengthening is an increasing function of the amount of disorder. The point of maximum strengthening is shifted towards higher values of p as the disorder increases. Four upper dashed lines visible on the right panel of Figure 1 refer to a ratio $\langle f_c^{\mathrm{GLS}}(p=0)\rangle/\langle f_c^{\mathrm{LLS}}(p=0)\rangle$ i.e. how many times an average GLS system with $p=0$ is stronger than an average LLS system with $p=0$. We can see that each LLS system, for its own value of p_c, reaches the above mentioned ratio.

The values of maximum strengthening together with the values of p related to them are reported in Table 1. There is a significant size effect observed for the LLS systems – the larger the system size the bigger the maximum strengthening.

3.2. The effect of elimination of elements by subcritical preloading

By applying $f_{\max}$ the array freezes in a stable state with N_{sub} ($N_{\mathrm{sub}}<N$) crushed pillars. Both $f_{\max}$ and N_{sub} are random variables. This raises a question: what is the value of f_c after the load $f_{\max}$ is released? To answer this question we have performed the following procedure. We have chosen a specific type of load transfer – GLS, LLS or a certain value of γ in the case of the RV rule. Then, for each system, we have simulated the loading process (in the presence of N intact pillars) to find values of

$f_{\max}$ and f_c^N i.e. maximum strength and critical load without preloading. Then, we have stored the configuration of the system after subcritical preloading, and for this configuration we have performed simulation leading to the calculation of f_c i.e. critical load for previously preloaded array. The above described procedure makes it possible to determine the ratio $\varphi = f_c/f_c^N$ which expresses strengthening/weakening of the preloaded array compared to its no preloaded counterpart.

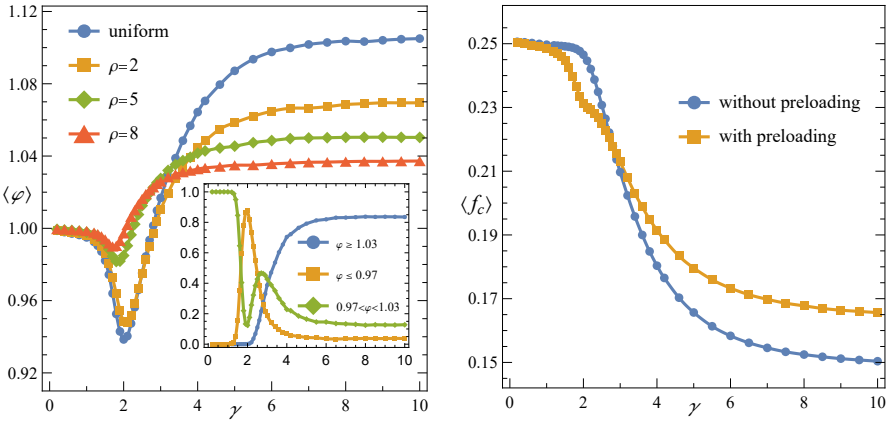

Fig. 2. (Left panel) The mean ratio $\langle\varphi\rangle$ as a function of parameter γ. Inset: the proportion of observations inside a given interval of φ in the case of uniform distribution. (Right panel) Mean critical load vs. γ for uniform distribution of pillar strength thresholds. Both panels concern systems of initial size $N = 100 \times 100$ pillars

To examine the behaviour of $\langle\varphi\rangle = \langle f_c\rangle/\langle f_c^N\rangle$ for different effective ranges of load transfer, we have explored the RV rule. In order to pass from long-range interactions to short-range interactions, we have tuned values of γ from 0 to 10. For $\gamma = 10$, the array behaves almost like the pure LLS system, whereas $\gamma = 0$ corresponds to the GLS rule. The transition point between the GLS-like and LLS-like behaviour has a value of about 2 ($\gamma_c \approx 2$) [10]. The results of simulations are graphically reported in the left panel of Figure 2. In the GLS-like regime ($\gamma \lessapprox 1$), the application of subcritical preloading has virtually no effect on the value of critical load. Then, as the effective range of interactions is decreased, we have noticed weakening of the systems. The weakening reaches its climax for $\gamma^* \in (1.7, 2)$ (depending on the distribution of pillar-strength-thresholds) i.e. values around γ_c. After the climax point, the ratio $\langle\varphi\rangle$ starts to grow rapidly with increasing γ, and then the increase of $\langle\varphi\rangle$ saturates. For all analyzed systems we observe strengthening in the regime of short-range interactions. However, the degree of strengthening is dependent on the distribution of pillar-strength-thresholds. The most significant strengthening concerns systems with a big amount of disorder of pillar-strength-thresholds.

It should be noted that the curves visible in the left panel of Figure 2 present the average behaviour. Even when the arrays are, on average, strengthened, some proportion of arrays may be weakened. To look closer into this, we arbitrarily divided φ into three intervals: $\varphi \leq 0.97$ (noticeable weakening), $0.97 < \varphi < 1.03$ (slight

change of critical load) and $\varphi \geq 1.03$ (noticeable strengthening). The effect of this division is shown in the inset of Figure 2. Up to $\gamma = 1.3$ there are no systems with $\varphi \geq 1.03$ or $\varphi \leq 0.97$. Furthermore, up to $\gamma = 2$ there are no systems with $\varphi \geq 1.03$. In the LLS-like regime, there is a dominance of $\varphi \geq 1.03$, although a small proportion of systems becomes noticeably weakened.

The right panel of Figure 2 shows the mean critical loads for systems before and after preloading. In both of these cases, the critical load is a decreasing function of γ. For the GLS rule ($\gamma = 0$), there is no effect of preloading ($\langle f_c^N \rangle = \langle f_c \rangle$), then $\langle f_c \rangle$ starts to go down faster than $\langle f_c^N \rangle$. The turning point is located around $\gamma = 2.8$. From this value of γ the preloading, on average, leads to the strengthening of the system. Hence, the subcritical preloading causes the growth of mean critical load in the significant presence of short-range interactions. When the long-range interactions dominate or short-range interactions are relatively weak, we observe a lack of strengthening or even a weakening of the systems.

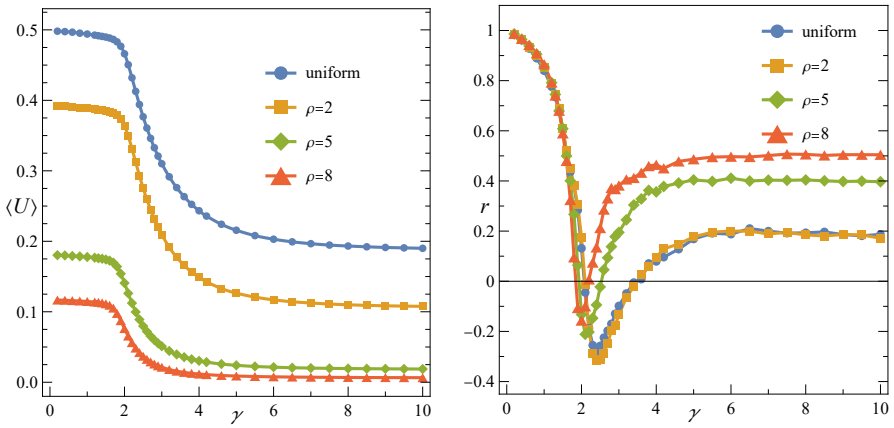

Fig. 3. (Left panel) Mean fraction of pillars crushed during subcritical preloading vs. γ. (Right panel) Correlation coefficient r between f_c and f_c^N as a function of γ. Both panels concern systems of initial size $N = 100 \times 100$ pillars

As the array is preloaded, the fraction $U = N_{\text{sub}}/N$ of its pillars is eliminated from the working elements. The mean value of U is dependent from distribution of $\{\sigma_{th}\}$ as well as from the effective range of interactions (see left panel of Fig. 3). Generally, $\langle U \rangle$ decreases as the effective range of interactions is reducing. Consider the regime of short-range interactions. Note that the bigger the dispersion of $\{\sigma_{th}\}$ is, the larger the $\langle U \rangle$ is, and the larger the mean strengthening $\langle \varphi \rangle$ is as well. Hence, elimination of a relatively large part of a population in the case of uniform distribution induces much more significant strengthening than in the case of $\rho = 8$, where only a very small part of the population is eliminated via subcritical preloading. The key point here is that, in the LLS-like regime, during the load redistributions strong load inhomogeneities arise due to load concentration in the weak regions.

Strongly disordered arrays contain a relatively large number of weak elements – as opposed to the arrays with small disorder. Following the preloading procedure,

the actual critical loading is performed by initially uniformly applied load on all intact pillars in the array in the absence of weak elements. Thus, the strongly disordered systems exhibit, on average, noticeable strengthening when the LLS-like rule governs the load transfer.

As in the GLS scenario, the application of subcritical preloading has no effect on the critical load, thus f_c and f_c^N exhibit a perfect linear relationship. For $\gamma > 0$, we employed Pearson's correlation coefficient r to statistically analyze the relationship between f_c and f_c^N. The results are presented in the right panel of Figure 3. For small values of γ, we observe a strong positive relationship. However, as the systems cross from long-range to short-range interactions, the values of r dramatically decrease to achieve negative values of r, and then there is a significant increase of r. In the short-range regime, the curve of r has a plateau-like shape, and the two analyzed values are lightly (or moderately) positively correlated.

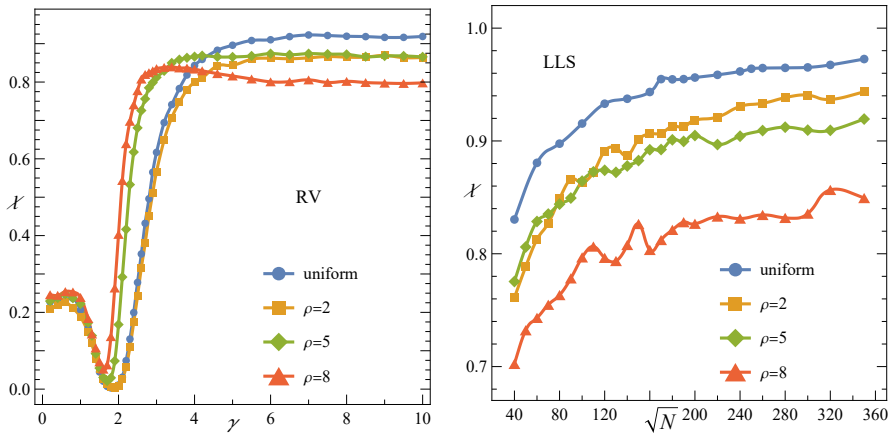

Fig. 4. (Left panel) Fraction of systems with $\varphi > 1$ as a function of γ. Initial system size $N = 100 \times 100$. (Right panel) Fraction of systems with $\varphi > 1$ vs. $\sqrt{N}$ when the LLS rule operates

Figure 4 illustrates the fraction χ of arrays that show strengthening ($\varphi > 1$) by subcritical preloading. Under the RV rule (left panel of Fig. 4), we observe that the majority of the arrays indicates strengthening only in the dominance of short-range interactions. From the right panel of Figure 4, we see that χ is an increasing function of N. The size effect is noticed under the LLS and LLS-like rules. However, in the right panel of Figure 4, some fluctuations are visible (especially for $\rho = 8$) due to sample size M, but the tendency is clear.

Taking short-range interactions into account, let's divide our sample population into two disjoint groups: arrays with enhanced critical loads ($\varphi > 1$) and arrays with deteriorated critical loads ($\varphi < 1$). The results of this partition are given in Figure 5 in the case of the RV rule with $\gamma = 10$. It is seen that the weakening concerns relatively stronger arrays and, after the preloading procedure, these arrays are among the weakest ones. This behaviour is observed in the case of short range interactions for all analyzed system disorders. It is noted that the loss of strength is, on average,

much smaller than the enhancement of critical load observed for the other arrays (see Table 2). Furthermore, also on average, critical loads f_c (after preloading) for systems with $\varphi < 1$ are bigger than critical loads f_c^N (before preloading) for systems with $\varphi > 1$.

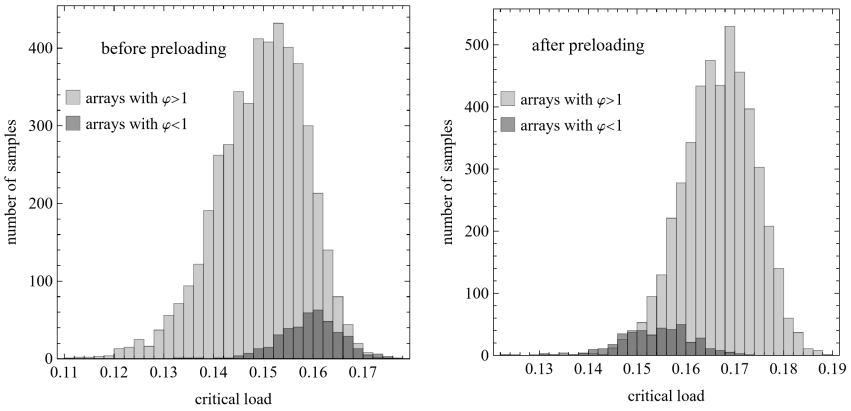

Fig. 5. Histogram of critical loads before (left panel) and after (right panel) subcritical preloading. Arrays with $N = 100 \times 100$ under the RV rule with $\gamma = 10$ and uniform distribution

Table 2. Fractions of arrays that exhibit strengthening and mean critical loads divided into two groups for chosen configurations in the presence of short-range interactions. Initial system size $N = 100 \times 100$

Load transfer	Fraction χ	Before preloading		After preloading	
		$\langle f_c^N \mid \varphi > 1 \rangle$	$\langle f_c^N \mid \varphi < 1 \rangle$	$\langle f_c \mid \varphi > 1 \rangle$	$\langle f_c \mid \varphi < 1 \rangle$
uniform					
$\gamma = 4$	0.843	0.1790	0.1877	0.1933	0.1814
$\gamma = 6$	0.910	0.1575	0.1668	0.1745	0.1615
$\gamma = 10$	0.919	0.1496	0.1595	0.1667	0.1536
LLS	0.915	0.1480	0.1573	0.1649	0.1515
$\rho = 2$					
$\gamma = 4$	0.800	0.3304	0.3444	0.3509	0.3342
$\gamma = 6$	0.862	0.3010	0.3154	0.3245	0.3062
$\gamma = 10$	0.864	0.2904	0.3047	0.3146	0.2956
LLS	0.863	0.2882	0.3031	0.3121	0.2937

In the last part of the section we return to the size effect observed in the LLS case. It is known that $f_c \sim 1/\ln N$. The formula for the mean critical load is given by

$$\langle f_c \rangle = \frac{\alpha}{\ln^{\beta}(\sqrt{N})} \tag{3}$$

where α and β are coefficients to be fitted. Figure 6 illustrates mean critical loads as a function of $\sqrt{N}$ for arrays before and after preloading. The strong size effect is evident for both scenarios. Values of the fitted parameters are included in Table 3.

As can be seen from the insets (of Fig. 6), the mean value of φ initially is an increasing function of N, however, it seems to gradually saturate for bigger system sizes.

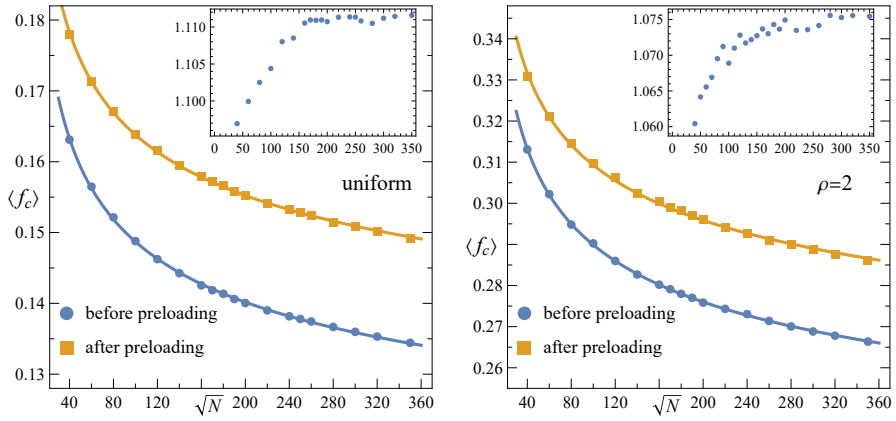

Fig. 6. Mean critical load as a function of $\sqrt{N}$ for the LLS systems. Solid lines represent fittings to the data using Eq. (3). Insets: ratio $\langle \varphi \rangle$ as a function of $\sqrt{N}$

Table 3. Values of fitted parameters α and β from the Eq. (3)

System disorder	Before preloading		After preloading	
	α	β	α	β
uniform	0.2831	0.4217	0.2939	0.3829
$\rho = 2$	0.4947	0.3500	0.5015	0.3165
$\rho = 5$	0.6799	0.2958	0.7068	0.2897
$\rho = 8$	0.7793	0.2661	0.8032	0.2631

4. Conclusion

We have numerically studied critical loads in suddenly loaded pillar arrays in the absence of some elements. In the first situation, it is assumed that a fraction p of weakest pillars is removed from the system prior to the actual critical loading procedure. Excluding the GLS rule, the mean critical load for all analyzed load transfer rules is an increasing function of p up to the transition point p_c. From the transition point, the mean critical load for a given configuration is the same irrespective of the applied load redistribution rule. Additionally, for $p > p_c$, the mean critical load starts to decrease. Therefore, the value of p_c determines the maximum strengthening of non-GLS arrays. The degree of strengthening and corresponding to it p_c are dependent on three factors: load transfer rule, system disorder and system size. The maximum strengthening is achieved in the case of the LLS rule and uniform distribution of pillar strength thresholds. In this case, we obtained an increase in strength of about two thirds.

In the second procedure, the actual critical loading of array is preceded by subcritical preloading. The number of pillars eliminated from the array during preloading is a random variable. In the context of critical load, the effect of preloading is neutral for the GLS rule ($\gamma = 0$). When the effective range of interactions is increased from $\gamma = 0$ to $\gamma^* \in (1.7, 2)$, we observe, on average, progressive weakening of the systems. Then, in the regime of short range interations, we have noticed strengthening of the arrays. The degree of strengthening/weakening and the exact position of γ^* are dependent on the distribution of pillar-strength-thresholds. Taking, for example $N \in \left(100^2, 300^2\right)$ and the LLS rule, the mean strengthening attains $\sim 11\%$ and $\sim 3.7\%$ for uniform distribution and Weibull distribution with $\rho = 8$, respectively.

References

[1] Park, J.E., Won, S., Cho, W., Kim, J.G., Jhang, S., Lee, J.G., & Wie, J.J. (2021). Fabrication and applications of stimuli-responsive micro/nanopillar arrays. *Journal of Polymer Science*, *59*, 1491.

[2] Chun, S., Pang, C., & Cho, S.B. (2020). A micropillar-assisted versatile strategy for highly sensitive and efficient triboelectric energy generation under in-plane stimuli. *Adv. Mater.*, *32*, 1905539.

[3] Jang, D., & Greer, J.R. (2010). Transition from a strong-yet-brittle to a stronger-and-ductile state by size reduction of metallic glasses. *Nature Materials*, *9*, 215-219.

[4] Shan, Z., Mishra, R., Syed Asif, S. et al. (2008). Mechanical annealing and source-limited deformation in submicrometre-diameter Ni crystals. *Nature Mater.*, *7*, 115-119.

[5] Taloni, A., Vodret, M., Costantini, G., & Zapperi, S. (2018). Size effects on the fracture of microscale and nanoscale materials. *Nature Reviews Materials*, *3*, 211-224.

[6] Hansen, A., Hemmer, P.C., & Pradhan, S. (2015). *The Fiber Bundle Model: Modeling Failure in Materials*. Wiley-VCH.

[7] Derda, T. (2022). Suddenly loaded arrays of pillars with variable range of load transfer. *Journal of Applied Mathematics and Computational Mechanics*, *21*(4), 16-27.

[8] Danku, Z., Pál G., & Kun, F. (2023). Size scaling of failure strength at high disorder. *Physica A: Statistical Mechanics and its Applications*, *624*, 128994.

[9] Roy, Ch., Kundu, S., & Manna, S.S. (2015). Fiber bundle model with highly disordered breaking thresholds. *Phys. Rev. E*, *91*, 032103.

[10] Hidalgo, R.C., Moreno, J., Kun, F., & Herrmann, H.J. (2002). Fracture model with variable range of interaction. *Physical Review E*, *65*, 046148.

[11] Biswas, S., & Goehring, L. (2016). Interface propagation in fiber bundles: Local, mean-field and intermediate range-dependent statistics. *New Journal of Physycs*, *18*, 103048.

[12] Roy, S., & Goswami, S. (2018). Fiber bundle model under heterogeneous loading. *J. Stat. Phys.*, *170*, 1197-1214.

[13] Derda, T., & Domanski Z. (2021). Survivability of suddenly loaded arrays of micropillars. *Materials*, *14*(23), 7173.

[14] Lee, J.-A., Lee, D.-H., Seok, M.-Y. et al. (2017). Significant strengthening of nanocrystalline Ni sub-micron pillar by cyclic loading in elastic regime.*Scr. Mater.*, *140*, 31-34.

[15] Wang, Z.-J., Li, Q.-J., Cui, Y.-N. et al. (2015). Cyclic deformation leads to defect healing and strengthening of small-volume metal crystals. PNAS 112, 13502-13507 .

[16] Derda, T., & Domanski, Z. (2020). Enhanced strength of cyclically preloaded arrays of pillars. *Acta Mech.*, *231*, 3145-3155 .